



# Effect of Cryptotanshinone on *Staphylococcus epidermidis* Biofilm Formation Under *In Vitro* Conditions

Ruiling Zu <sup>1,2</sup>, Hui Yi <sup>1,3</sup>, Yuling Yi <sup>1</sup>, Jiangyan Yong <sup>1</sup> and Yan Li <sup>1,\*</sup>

<sup>1</sup>School of Medical Technology, Chengdu University of Traditional Chinese Medicine, Chengdu, China

<sup>2</sup>Department of Clinical Laboratory, Sichuan Cancer Hospital and Institute, Chengdu, China

<sup>3</sup>Department of Clinical Laboratory, Wenjiang District People's Hospital of Chengdu, Chengdu, China

\*Corresponding author: School of Medical Technology, Chengdu University of Traditional Chinese Medicine, Chengdu, China. Email: 1067267085@qq.com

Received 2018 September 04; Accepted 2019 March 31.

## Abstract

**Background:** *Staphylococcus epidermidis* causes prosthetic valve endocarditis, urinary tract infection, and implant-related infections. These are difficult to treat often due to drug resistance, particularly because *S. epidermidis* biofilms are inherently resistant to most antibiotics. *Salvia miltiorrhiza* is a kind of sichuan-specific medicinal herb, and has effective ingredients, such as cryptotanshinone. Cryptotanshinone was demonstrated to have anti-microbial properties and no resistance.

**Objectives:** The current study investigated the effects of cryptotanshinone on *S. epidermidis* biofilm formation, and found new agents controlling *S. epidermidis* biofilm formation and resistance caused by biofilm.

**Methods:** The effects were further analyzed by crystal violet assay (CV), 2, 3-bis [2-methoxy-4-nitro-5-sulfophenyl]-2H-tetrazolium-5-carboxanilide inner salt assay (XTT), and scanning electron microscopy (SEM). The qRT-PCR assay was used to determine the expressions of biofilm key genes, including *icaA*, *atlE*, *aap* and *luxS*.

**Results:** The amount treated by cryptotanshinone was reduced compared with the non-treating group, so did the metabolic activity inside the biofilm. Even the micro-structure was destroyed with cryptotanshinone. The expressions of biofilm key genes, including *icaA*, *atlE*, *aap*, and *luxS*, were down-regulated by cryptotanshinone.

**Conclusions:** There is new insight that cryptotanshinone could inhibit immature biofilms and the down-regulations of *icaA*, *atlE*, *aap*, and *luxS* might explain this inhibitory effect.

**Keywords:** Cryptotanshinone, *Staphylococcus epidermidis*, Biofilm

## 1. Background

*Staphylococcus epidermidis* is an important cause of hospital-acquired opportunistic infection, accounting for more than half of implant-associated bacterial infection (1). Recently, *S. epidermidis* accounted for 19.3% to 30.1% of many catheter-related blood stream infections (CRBSI), caused by the most common implant catheter (2, 3). Furthermore, *S. epidermidis* was also estimated to occur in more than 50% of joint-implant infections (4). The strong implant-adhering and biofilm-forming ability of *S. epidermidis* were blamed for these infections (5).

Biofilms comprise of microorganisms, which are not only bacterial colonies yet also biological systems. It has been documented that biofilms allow *S. epidermidis* to tolerate high concentrations of antibiotics, protect bacteria from host immune attacks and other environmental stresses, and facilitate spread of bacterial infection (6-8). As a result, treatment of biofilm-associated infections is

very challenging and often involves overuse of antibiotics, which may cause the development of resistance. The formation of *S. epidermidis* biofilms includes adhesion, cell accumulation, and maturation phases (9), therefore, the effects might be different when the antibacterial agents intervene in different phases of biofilms. Clearly, it would be beneficial to identify new agents that can prevent biofilm formation and dissemination.

Tanshinone is the major chemical compound isolated from the root of the Asian medicinal herb, *Salvia miltiorrhiza* bunge (Danshen) (10, 11). Known as Danshen in China and first recorded as a "top-grade" herb in Sheng Nong's Herbal Classic (A.D. 102 - 200), *S. miltiorrhiza* has been used for treating cardiovascular diseases and neurasthenic insomnia for thousands of years in traditional Chinese medicine (12-16). In the recent years, there has been extensive research on chemical constituents in order to determine the effectiveness of application in modern medicine. Tanshinone was proved to exhibit strong antimicrobial ac-

tivities against a broad range of Gram-positive and Gram-negative bacteria as well as other microorganisms, including viruses (17-19), though its mechanisms of antimicrobial action remain poorly understood. Based on studies of *S. epidermidis* (18) and *S. aureus* (19), tanshinone was used to inhibit the formation of *S. epidermidis* biofilms in this research. However, there has been no report of effects of tanshinone on biofilm formation in any bacteria.

## 2. Objectives

The researchers' previously published report on Chinese participants revealed that tanshinone displayed antibacterial and anti-biofilm activities on *S. epidermidis* (20). Additionally, the aim of this research was to find the most potent inhibitor against *S. epidermidis* among all tanshinone compounds. The primary goal of this study was to characterize the effects of tanshinone on different phases of biofilm formation in *S. epidermidis*.

## 3. Methods

### 3.1. Bacterial Strains

A biofilm positive *S. epidermidis* strain SE 1457 was kindly provided by Qu Di, Fudan University, Shanghai, China (21). The strains were maintained in tryptic soy broth media (TSB, Baltimore, MD, USA).

### 3.2. Growth Curves

*Staphylococcus epidermidis* biofilms were grown on 96-well plates at 37°C in 200- $\mu$ L biofilm-inducing medium per well with a starting inoculum of  $2 \times 10^6$  CFU/mL. During the time points (6, 12, 18, 24, 30, 36, 42, and 48 hours) biofilms were determined by crystal violet staining (crystal violet (CV) assay) and XTT assay (22, 23). For the CV assay, the medium was discarded and the plate was washed three times with PBS, and then stained with 200  $\mu$ L of 0.5% (w/v) crystal violet, as described previously (24). The bound crystal violet was released from stained cells by adding 75% ethanol and the absorbance of the solution was measured at 590 nm in a microplate reader (KHB, ST-360, Shanghai, CHN). For XTT assay (25), the wells were filled with XTT work liquid (Nanjing KeyGen Biotech. Co., Ltd.) and incubated for an additional two hours in the dark. The absorbance was measured at 450 nm.

### 3.3. Antimicrobial Agents

Cryptotanshinone, dihydrotanshinone, tanshinone I, and tanshinone IIA were purchased from Chengdu Preferred Biological Technology (Co., Ltd., Chengdu, China),

and dissolved in DMSO and filtered through 0.22  $\mu$ m Millipore filters (Sartorius Co., NY, USA). Vancomycin, ampicillin, oxacillin, cefazolin, and erythromycin were purchased from National Institutes for Food and Drugs Control (Beijing, China) and dissolved in appropriate solvents, according to Clinical and Laboratory Standards Institute (26).

### 3.4. Minimum Inhibitory Concentrations (MICs)

The MICs of the most abundant constituents of tanshinone and antibiotics, including cryptotanshinone, dihydrotanshinone, tanshinone I, tanshinone IIA, vancomycin, ampicillin, oxacillin, cefazolin, and erythromycin, were determined by the standard micro-titre broth dilution method using 96-well microplates (26). In each well, a 100- $\mu$ L microbial culture ( $5 \times 10^5$  CFU/mL) was mixed with 100  $\mu$ L of serially diluted tanshinones or antibiotics (0.25, 0.5, 1, 2, 4, 8, 16, 32, 64 or 128  $\mu$ g/mL) or solvent, as a control. Microplates were incubated at 37°C for 24 hours. Each sample was tested in triplicates in at least three independent experiments. The MICs were defined as the lowest concentration that yielded no visible bacterial growth after 24 hours.

### 3.5. Minimum Biofilm Inhibitory Concentrations (MBIC)

Biofilms culture was started as described in growth curves, and the time point of biofilm growth was ascertained according to the growth curves. *Staphylococcus epidermidis* biofilms were grown on 96-well plates at 37°C in 200  $\mu$ L biofilm-inducing medium per well with a starting inoculum of  $2 \times 10^6$  CFU/mL. After culturing for 24 hours, the medium was replaced with 100  $\mu$ L of serially diluted tanshinones or antibiotics (0.25, 0.5, 1, 2, 4, 8, 16, 32, 64 or 128  $\mu$ g/mL) or no drug, as the control. Each sample was tested in triplicates in at least three independent experiments. The MBICs were defined as the lowest agent concentration with no visible turbidity after 24 hours (27, 28).

### 3.6. Effects of Cryptotanshinone on Biofilm Determined by Crystal Violet Staining (CV Assay)

The time points of different phases of biofilm formation were ascertained by the growth curves. The antimicrobial agents and their concentrations were selected according to MICs and MBICs. After culturing for 6, 24 or 48 hours, the medium was replaced with 200  $\mu$ L of TSB, containing 128  $\mu$ g/mL cryptotanshinone, 32  $\mu$ g/mL cryptotanshinone, 32  $\mu$ g/mL vancomycin or no inhibitor (control). After incubation for an additional 24 hours, the medium was discarded and the plate was washed three times with PBS, and then determined by CV assay, as described previously in growth curves (24).

### 3.7. Effects of Cryptotanshinone on Biofilm Metabolic Activities (XTT Assay)

The metabolic activity of biofilms formed by *S. epidermidis* was measured using the tetrazolium salt (XTT) reduction assay as previously described in growth curves. Briefly, after biofilms were pre-grown for 6, 24 or 48 hours, as described above, in the CV assay, the culture medium was changed to 200  $\mu$ L Mueller-Hinton broth (MHB) in the presence of 128  $\mu$ g/mL cryptotanshinone, 32  $\mu$ g/mL cryptotanshinone, 32  $\mu$ g/mL vancomycin or without an inhibitor (control) (25).

### 3.8. Effects of Cryptotanshinone on Biofilm Micro Structure Determined by Scanning Electron Microscopy (SEM Assay)

To determine the effects of cryptotanshinone on biofilm microstructure, *S. epidermidis* biofilms were formed on glass coverslips in six-well plates at 37°C and challenged with cryptotanshinone, vancomycin, or no inhibitor (control). After incubation for 6, 24 or 48 hours, the coverslip was rinsed three times with PBS, followed by gradual dehydration in ethyl-alcohol (30%, 50%, 70%, 70%, 80%, 90% and 100% in v/v). Then, the coverslip was rinsed with tert-Butyl alcohol, and dried in vacuum. After metal spraying, the biofilm was observed by SEM (Inspect F, FEI, USA). Ten views were observed, and the diameter of each view was fixed as 10  $\mu$ m. The amount of bacteria and morphology was visualized in each view (29, 30).

### 3.9. Effects of Cryptotanshinone on Expression of Key Genes Involved in Biofilm Formation Determined by Quantitative Reverse-Transcription PCR (qRT-PCR Assay)

It has been reported that *icaA*, *atlE*, *aap*, and *luxS* are the key genes involved in biofilm formation in *S. epidermidis* (31). To determine the effects of cryptotanshinone on mRNA expression of these genes during biofilm formation in *S. epidermidis*, real-time qRT-PCR was performed (32). Briefly, biofilms were grown on six-well plates in the presence of cryptotanshinone or vancomycin or without any inhibitor (control), as described above. Cell pellets were harvested and washed three times with PBS treated with 0.1% diethylpyrocarbonate (DEPC, Sangon, Shanghai, CHN). Total RNA was extracted using the TRIzol® RNA isolation kit (Invitrogen, Madison, WI, USA). The cDNA was synthesized from total RNA using the TransScript II All-in-One First-Strand cDNA Synthesis SuperMix for the qPCR system (TransGen Biotech, Beijing, CHN). Primers specific for *S. epidermidis* *icaA*, *atlE*, *aap*, and *luxS* as well as 16S rRNA gene (internal control) were designed using the NCBI Primer-BLAST (<https://www.ncbi.nlm.nih.gov/tools/primer-blast/>) and synthesized by Sangon Biotech (Shanghai, CHN) (Table 1).

**Table 1.** Primers Used for RT-PCR in This Study

Gene	Primer Sequence (5' - 3')	Product Length, bp
<b>16SrRNA</b>		194
F	CTCGTGTGCTGAGATGTTGG	
R	TTCGCTGCCCTTGTATTG	
<b>icaA</b>		209
F	TGGTTGTATCAAGCGAAGTCA	
R	CAGGCACTAACATCCAGCATA	
<b>atlE</b>		144
F	TGGTCTATATTCTATTGCTTGGGG	
R	CCTGTTCTGTATTGACTGTTCGG	
<b>aap</b>		165
F	AAGCCCCTACAAGAAATGACCTA	
R	TGCTTAATAAGGACATAAACGGAGA	
<b>luxS</b>		226
F	TGACATTCGTTTCAAACAGCCC	
R	ATTACAAGCTGGGACTTCGCT	

The qRT-PCR was performed using the TransStart Green qPCR SuperMIX (Transgen, Beijing, China) and the qTower® real-time PCR system (Analytik Jena, GER) following the instructions of the manufacturers. The thermo cycling parameters included an initial denaturation at 94°C for 30 seconds, followed by 40 cycles of 94°C for 5 seconds, 53°C for 15 seconds, and 72°C for 10 seconds. Melting-curve analysis was started from initial temperature of 60°C to 95°C, with a gradual increase of 1°C every six second. Specificity of the primers was confirmed by melting curve analysis. The resulting threshold cycle (CT) values were normalized to the CT value of the 16S rRNA gene. Relative expression fold changes were calculated by the  $2^{-\Delta\Delta ct}$  formula.

### 3.10. Statistical Analysis

Data from the CV, XTT, and qRT-PCR assays were expressed as mean values  $\pm$  standard deviations (SD), and analyzed by the analysis of variance (ANOVA) method, using the SPSS 19.0 software (SPSS Inc., Chicago, IL).  $P < 0.05$  was considered statistically significant.

## 4. Results

### 4.1. Susceptibility and Biofilm Formation

The MICs and MBICs are summarized in Table 2. Overall, 2  $\mu$ g/mL of cryptotanshinone could inhibit *S. epidermidis* growth and 32  $\mu$ g/mL of cryptotanshinone could inhibit biofilms. Compared with other compounds from tanshinone, cryptotanshinone showed the strongest effect

on *S. epidermidis* biofilms. The MICs of antibiotics were from 0.125  $\mu\text{g}/\text{mL}$  to 2  $\mu\text{g}/\text{mL}$ , except erythromycin. However, the MBICs of antibiotics were above 128  $\mu\text{g}/\text{mL}$ , except vancomycin. Compared with other antibiotics, only vancomycin could be considered as having an inhibitory effect on *S. epidermidis* biofilms. Therefore, 32  $\mu\text{g}/\text{mL}$  of cryptotanshinone, 32  $\mu\text{g}/\text{mL}$  vancomycin and a higher concentration (128  $\mu\text{g}/\text{mL}$ ) were selected for the following research.

The formation of biofilms is a dynamic process defined as three phases that are adhesion, accumulation, and mature phases. These phases are indicated on the growth curves. The CV assay reflected the matrices of biofilm and the XTT assay reflected the bacteria activities inside biofilms (32). During the adhesion phase, the bacteria adhered to the surface and colonized, which thickened the matrices. From the beginning to 12 hours, matrices of biofilms grew rapidly in the exponential phase and so did bacteria inside biofilms (Figures 1 and 2), which could present the *S. epidermidis* initial adherence to the surface.

In the accumulation phase, bacteria accumulated with each other and established a three-dimensional, multi-cellular, and multi-layered architecture, in which matrices did not get thick, while the bacteria stayed active. Matrices stayed in the lag phase, which lasted from 12 hours to 24 hours, while metabolic activities stayed in the lag stage from 18 hours to 30 hours. Once the structure frame was built, the biofilms were back growing and became stronger. Therefore, matrices were growing from 24 to 42 hours, and metabolic activities were back growing from 30 hours to 42 hours, which was not as fast as the first stage. Therefore, biofilms were in the accumulation phase from

12 to 42 hours. When biofilms entered the mature phase, bacteria kept a balance inside the biofilm. From 42 to 66 hours, both matrices and metabolic activities grew to the stationary stage. Then, biofilms started to decline because of the nutrient depletion and death of bacteria. Therefore, the time point 6, 24 or 48 hours, respectively, represented the three phases of biofilm formation.

#### 4.2. Effects of Cryptotanshinone on Biofilm Formation Based on the CV Assay

The inhibitory effects on *S. epidermidis* biofilm formation were determined using two concentrations of cryptotanshinone (32  $\mu\text{g}/\text{mL}$  and 128  $\mu\text{g}/\text{mL}$ ) or vancomycin (32  $\mu\text{g}/\text{mL}$ ) in the CV assay, in which the optical density was 590 ( $A_{590}$ ) units and reflected the amount of biofilm matrices formed (Figure 3). In the first phase compared to no treatment control (with  $A_{590}$  of  $1.317 \pm 0.02$ ), there was a statistically significant decrease in the amount of biofilm matrices formed in the 128  $\mu\text{g}/\text{mL}$  cryptotanshinone-treated group (with  $A_{590}$  of  $0.55 \pm 0.02$ ,  $P < 0.05$ ) as well as the 32  $\mu\text{g}/\text{mL}$  cryptotanshinone-treated group (with  $A_{590}$  of  $0.725 \pm 0.02$ ,  $P < 0.05$ ). Compared with the vancomycin-treated group (with  $A_{590}$  of  $0.128 \pm 0.01$ ), the amount of biofilm matrices formed in the two cryptotanshinone-treated group was much higher ( $P < 0.05$ ).

In the second phase, the amount of biofilm matrices formed in the 128  $\mu\text{g}/\text{mL}$  cryptotanshinone-treated group (with  $A_{590}$  of  $1.45 \pm 0.0$ ,  $P < 0.05$ ) significantly decreased compared to the no treatment control (with  $A_{590}$  of  $1.753 \pm 0.08$ ), and the same was found in the vancomycin-treated group (with  $A_{590}$  of  $1.296 \pm 0.06$ ,  $P < 0.05$ ). There was no significant difference in the amount of biofilm matrices formed between the low concentration group (with  $A_{590}$  of  $1.439 \pm 0.21$ ,  $P > 0.05$ ) and the control. Compared with the vancomycin-treated group, the amount of biofilm matrices formed in the 128  $\mu\text{g}/\text{mL}$  cryptotanshinone group was also higher.

In the third phase, compared to the no treatment control (with  $A_{590}$  of  $1.88 \pm 0.04$ ), the amount of biofilm matrices formed in the 128  $\mu\text{g}/\text{mL}$  cryptotanshinone-treated group (with  $A_{590}$  of  $1.193 \pm 0.06$ ,  $P < 0.05$ ) was decreased significantly, and, it was less than the 32  $\mu\text{g}/\text{mL}$  vancomycin-treated group (with  $A_{590}$  of  $1.478 \pm 0.06$ ). However, there was no significant decrease in the 32  $\mu\text{g}/\text{mL}$  cryptotanshinone-treated group (with  $A_{590}$  of  $1.879 \pm 0.05$ ,  $P < 0.05$ ).

#### 4.3. Effects of Cryptotanshinone on Biofilm Metabolic Activities Based on the XTT Assay

In the XTT assay, metabolic activities were expressed as optical density 450 ( $A_{450}$ ) (Figure 4). In the first phase,

**Table 2.** Antimicrobial Susceptibility Testing Results

Antimicrobial Agents	MIC, $\mu\text{g}/\text{mL}$	MBIC, $\mu\text{g}/\text{mL}$
<b>Tanshinone</b>		
Cryptotanshinone	2	32
Dihydrotanshinone	8	128
Tanshinone I	8	128
Tanshinone IIA	> 128	> 128
<b>Antibiotics</b>		
Vancomycin	2	32
Ampicillin	1	128
Oxacillin	1	> 128
Cefazolin	0.125	> 128
Erythromycin	> 128	> 128

Abbreviations: MBIC, minimum biofilm inhibitory concentrations; MIC, minimum inhibitory concentration.

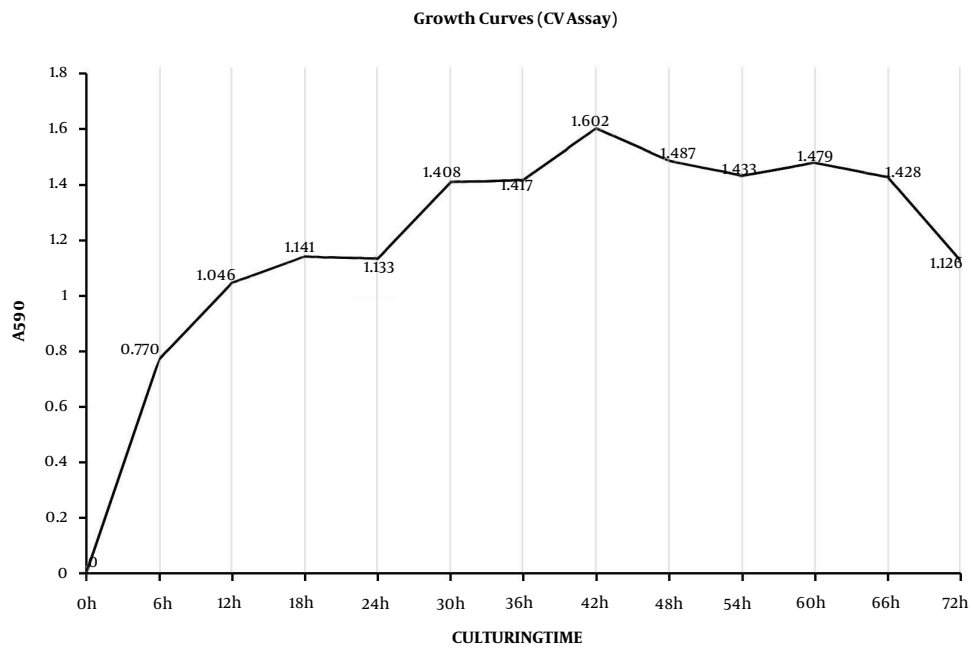


**Figure 1.** The growth curves of *Staphylococcus epidermidis* biofilm formation detected by CV assay

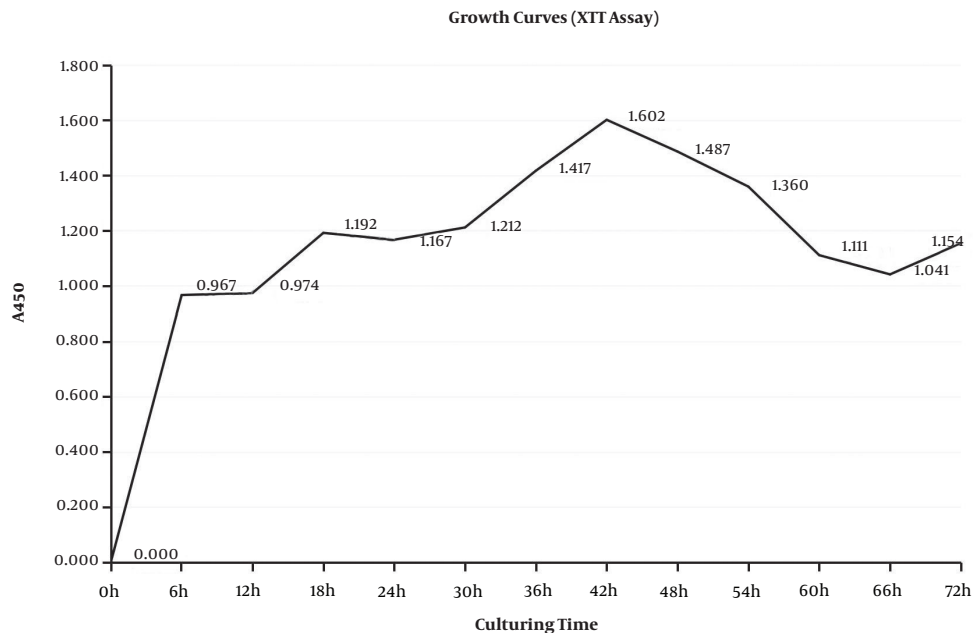


**Figure 2.** The growth curves of *Staphylococcus epidermidis* biofilm formation detected by XTT assay

the biofilm metabolic activity was reduced to 61.16% in the 128  $\mu\text{g}/\text{mL}$  cryptotanshinone-treated group ( $A_{450} = 0.574 \pm 0.04$ ,  $P < 0.05$ ), 24.97% in the 32  $\mu\text{g}/\text{mL}$  cryptotanshinone-treated group ( $A_{450} = 1.109 \pm 0.04$ ,  $P < 0.05$ ) and 81.53%

in the vancomycin-treated group ( $A_{450} = 0.273 \pm 0.02$ ,  $P < 0.05$ ) compared to the untreated control group (with  $A_{450}$  of  $1.478 \pm 0.05$ ). There was a significant difference in the biofilm metabolic activity among these three treated



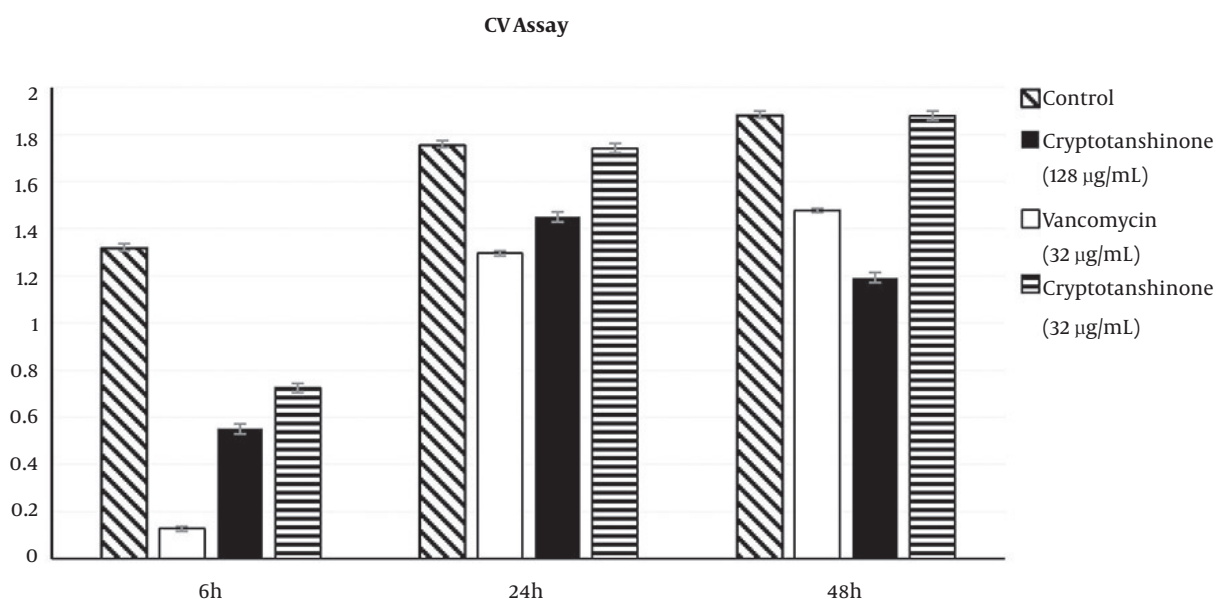


**Figure 3.** *Staphylococcus epidermidis* biofilm matrices inhibition after 6, 24 and 48 hours by cryptotanshinone at concentrations of 32 µg/mL and 128 µg/mL

groups ( $P < 0.05$ ). In the second stage, the metabolic activities were 34.81% for vancomycin ( $A_{450} = 0.612 \pm 0.06$ ), while the activities were 44.94% and 75.94% for cryptotanshinone at the concentration of 128 µg/mL and 32 µg/mL ( $A_{450} = 0.79 \pm 0.04$  and  $A_{450} = 1.335 \pm 0.06$ ). In the third stage, there was a slight inhibition of cryptotanshinone (128 µg/mL, with  $A_{450} = 1.185 \pm 0.05$ ) and vancomycin ( $A_{450} = 1.085 \pm 0.03$ ) ( $P < 0.05$ ), while there was no inhibitory effect for cryptotanshinone (32 µg/mL,  $A_{450} = 1.322 \pm 0.04$ ) and only a slight inhibitory effect was observed ( $P > 0.05$ ).

#### 4.4. Effects of Cryptotanshinone on Biofilm Micro Structure Based on SEM

The 10 views equably showed the biofilms, therefore one representative image was picked, as shown in Figure 5. The image of the control sample demonstrates the complex structure of the biofilm filled with cells. In the sight with the same diameter, a significant reduction in bacteria amount was revealed in the image of the cryptotanshinone sample, especially at a higher concentration (128 µg/mL) in the first and third phase, and no reduction in the second phase.

#### 4.5. Effects of Cryptotanshinone on Expression of Key Genes Involved in Biofilm Formation Based on qRT-PCR

The relative expression levels of four key genes (*icaA*, *atlE*, *aap*, and *luxS*) known to be involved in *S. epidermidis* biofilm formation were assessed by qRT-PCR, including 16S

rRNA gene as an internal control for normalization (Figure 6). The expressions of controls were set as “1”, and the expressions of other groups were correspondingly calculated according to the control. The expressions of *ica*, *atlE*, *aap*, and *luxS* were down-regulated by cryptotanshinone (128 µg/mL and 32 µg/mL) and vancomycin in the first and second phase ( $P < 0.05$ ). However, in the third phase, the expressions of the four genes were down-regulated by cryptotanshinone (128 µg/mL) and vancomycin, while up-regulated by cryptotanshinone (32 µg/mL) ( $P < 0.05$ ).

## 5. Discussion

Biofilm formation is the main pathogenic factor of *S. epidermidis*. Biofilm formation was a dynamic process always described in three phases: Initial adhesion (1 to 12 hours), intercellular accumulation (12 to 42 hours), and mature phase (42 to 66 hours). The development of biofilms may allow for aggregation of cell colonies to be increasingly resistant to antibiotics. The antimicrobial agents may show the different extent of inhibitory effect in the different phases of biofilm formation. Therefore, the agents intervened with the three phases of biofilms in this research.

Usually, vancomycin, ampicillin, oxacillin, cefazolin, and erythromycin were common antibiotics used to treat Gram-positive organisms infection (26). In this research, planktonic *S. epidermidis* could be inhibited by vancomycin, ampicillin, oxacillin, and cefazolin, however, *S.*

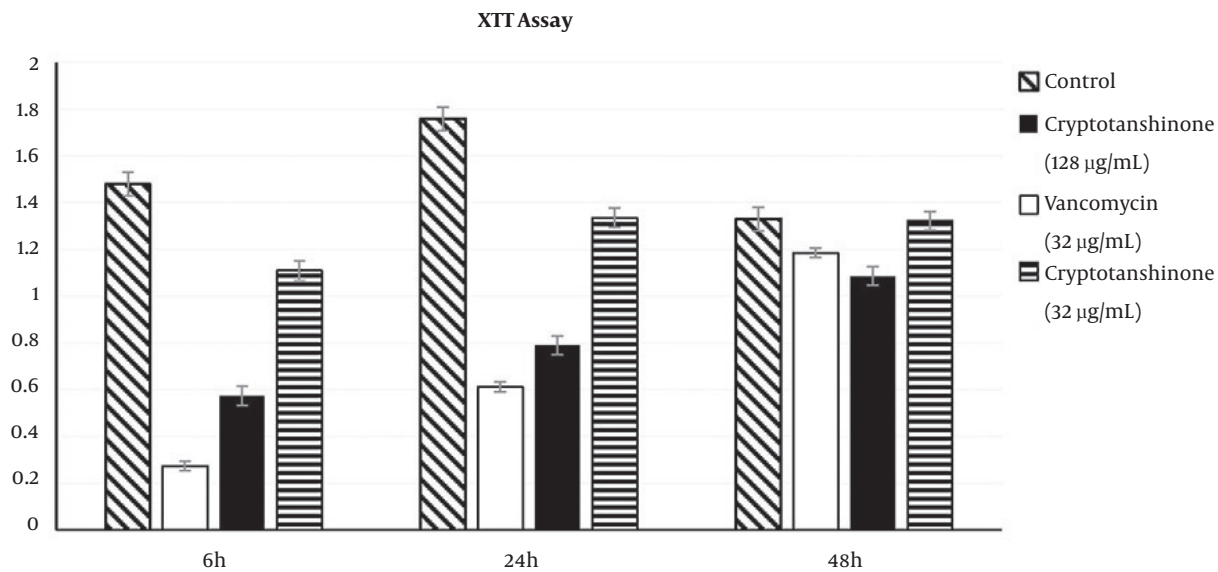


**Figure 4.** The reduction of metabolic activities inside *Staphylococcus epidermidis* biofilm after 6, 24 and 48 hours by cryptotanshinone at concentrations of 32 µg/mL and 128 µg/mL

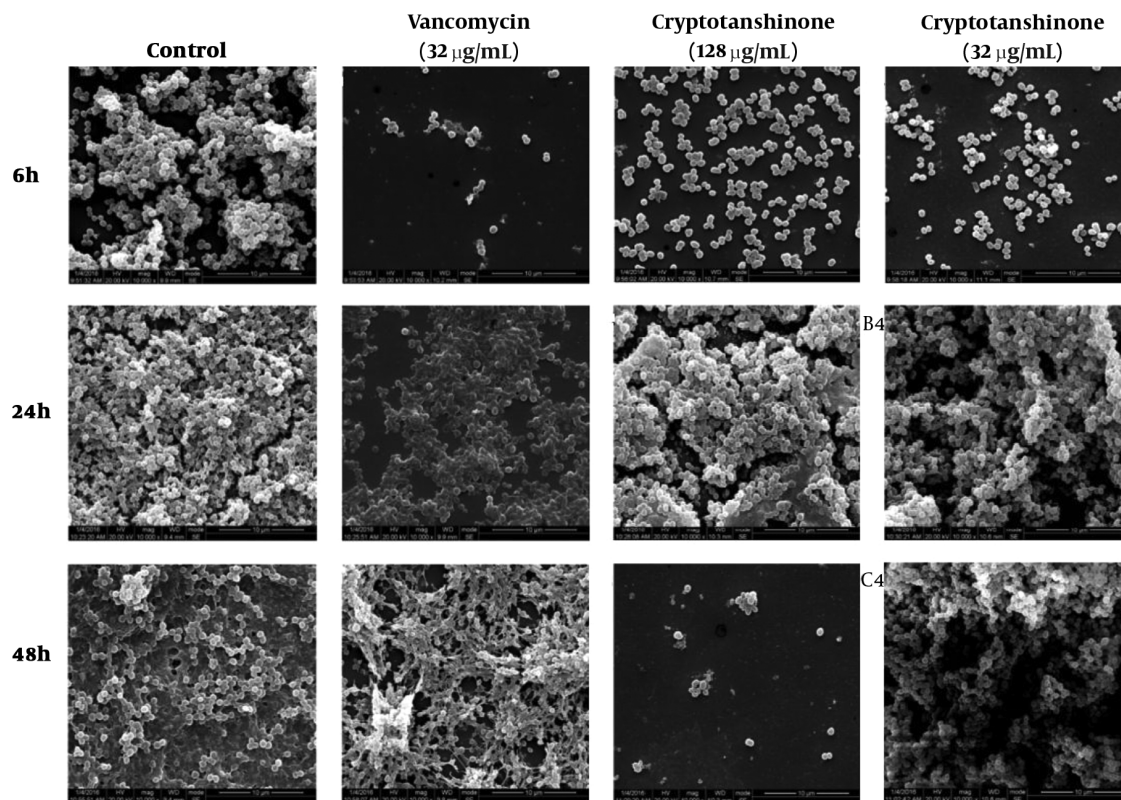


**Figure 5.** SEM images of *Staphylococcus epidermidis* 1457 biofilms at three different phases. The biofilms were formed on the cover glass slips on 6-well plates treated with different drugs and concentrations.

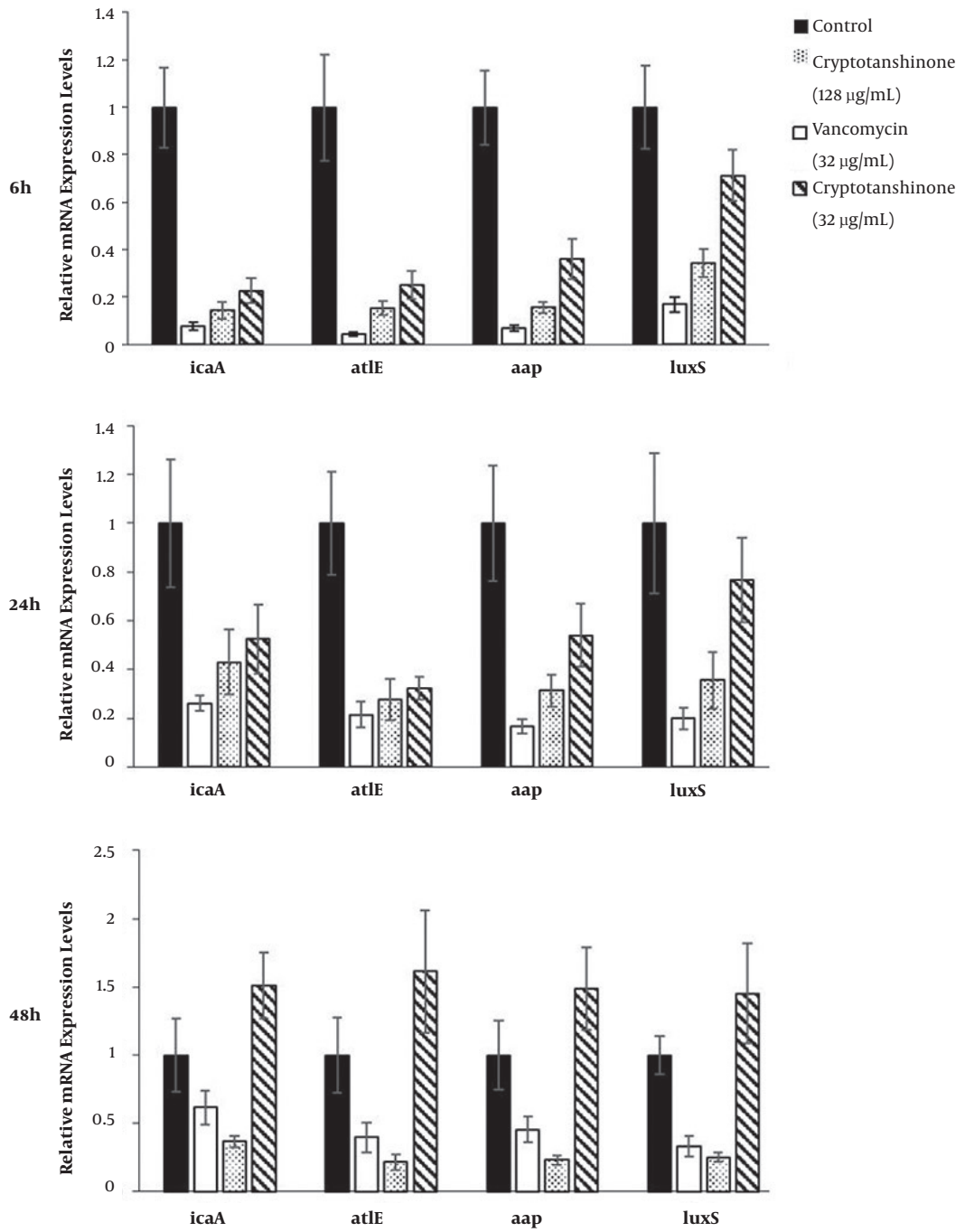


**Figure 6.** Relative mRNA expression levels of the key genes in three different phase of biofilm formation; Bars and error bars represent the mean  $\pm$  SD of results. Results were compared relatively on the basis of control group expression quantity, which was regarded as "1".



*epidermidis* biofilms showed less susceptibility to these antibiotics. Based on MBICs, only vancomycin inhibited *S. epidermidis* biofilms. At present, vancomycin is commonly used for the treatment of serious infections by Gram-positive bacteria unresponsive to other antibiotics. However, vancomycin has traditionally been considered a nephrotoxic and ototoxic drug, and may increase with drug-resistance. Therefore, vancomycin is always considered as the last resort for the treatment of Gram-positive bacteria. If a new agent that is nontoxic and can inhibit *S. epidermidis* biofilms as strong as vancomycin was found, it could make great sense.

In the past few years, Danshen and its medical products have become popular around the world because of the broad-spectrum therapeutic effects of this herb and its lack of apparent adverse effects (11, 33). If tanshinone could inhibit the formation of *S. epidermidis* biofilms, it might be a better choice than vancomycin. Based on inhibitory testing results, the researchers found that cryptotanshinone had the strongest anti-biofilm effect among the extracts from tanshinone. The activities of cryptotanshinone-inhibiting *S. epidermidis* biofilm *in vitro* was also examined. The CV assay, XTT assay results, and SEM images showed significant reduction in biofilm matrices, metabolic activities, and morphological changes of *S. epidermidis* in the intervention of cryptotanshinone as well as vancomycin.

When the cryptotanshinone (128  $\mu\text{g}/\text{mL}$  and 32  $\mu\text{g}/\text{mL}$ ) was added at the initial adhesion stage, the matrices were decreased, the cellular activities inside biofilms were reduced, and the structures of biofilms were destroyed. It was earlier reported that in the adhesion phase, polysaccharide intercellular adhesion (PIA) is made up of sulfated polysaccharides, which allows other bacteria to bind to the already existing biofilms, creating a multilayer biofilm. However, PIA is a major part of the extracellular matrixes synthesized by the gene products of the *ica* operon (34), which was down-regulated by cryptotanshinone. As a consequence, the cryptotanshinone might decrease the amount of PIA further to decrease the matrices though down-regulating the *ica* operon.

Along with adhesion, the bacteria produced accumulation-associated rotein (Aap) and autolysin E (AtLE) coded by *aap* and *atlE* previously, and contributes to intercellular connections and surface attachment (5, 35). On the whole, PIA forms the major part of the matrixes of biofilms together with ATLE and AAP. When the cryptotanshinone (128  $\mu\text{g}/\text{mL}$ ) intervened in the adhesion and accumulation phases, the expressions of *atlE* and *aap* were decreased, and the polysaccharides and proteins were accordingly reduced, so it was difficult for the bacteria to adhere on the surface or accumulate with each other. Thus, the matrixes of biofilms were fewer, the biofilms

were thinner, and same in the metabolic activities of biofilms. Therefore, down-regulation of these genes by cryptotanshinone (128  $\mu\text{g}/\text{mL}$ ) is consistent with its effects on biofilm foundations.

In mature biofilms, bacteria monitor their own population density or that of other populations by recognizing local concentrations of chemical molecules, according to the QS system, such as the *luxS* system (36-38). The transcript levels of *luxS* in mature biofilms treated with cryptotanshinone (128  $\mu\text{g}/\text{mL}$ ) were also found to be reduced, and accordingly the metabolic activities inside biofilms were decreased. However, when the biofilms grew mature, the cryptotanshinone (32  $\mu\text{g}/\text{mL}$ ) could not inhibit the growth anymore, which indicated cryptotanshinone had a dose-dependent effect on *S. epidermidis* biofilms.

### 5.1. Conclusions

Above all, these results are the first preclinical proofs of evidence for cryptotanshinone capable of inducing *S. epidermidis* biofilm degradation. Furthermore, cryptotanshinone inhibited three phases of *S. epidermidis* biofilm, same as vancomycin, due to the down-regulation of biofilm-related genes, such as *ica*, *atlE*, *aap*, and *luxS*. Therefore, the cryptotanshinone inhibits biofilm formation of *S. epidermidis* via decreasing PIA, ATLE, and AAP production with a dose-dependent effect. Hence, cryptotanshinone has a broad prospect in treating many kinds of infections not only caused by *S. epidermidis* biofilms. The researchers propose further *in vivo* studies on the combination of cryptotanshinone and antibiotics, which will provide new insights into the potential therapeutic effects of cryptotanshinone in the treatment of *S. epidermidis* biofilm-associated infections.

### Acknowledgments

*Staphylococcus epidermidis* 1457 (biofilm positive) were presented by Professor Qu Di (Fudan University, Shanghai, China).

### Footnotes

**Authors' Contribution:** Conception and design: Yan Li and Hui Yi. Experiment: Ruiling Zu and Hui Yi. Data analysis and interpretation: all authors. Manuscript writing: all authors. Final approval of manuscript: all authors. Accountable for all aspects of the work: all authors.

**Conflict of Interests:** The authors declare that there was no conflict of interest regarding the publication of this article.

**Ethical Considerations:** The research did not refer to the animal model or clinical trial, therefore the school did not require an ethical statement. The researchers will apply for ethical statements in future work.

**Financial Disclosure:** There is nothing to disclose.

**Funding/Support:** This work was supported by the Department of Sciences and Technology of Sichuan province under grant number 2015JY0159.

## References

- Kuehl R, Brunetto PS, Woischnig AK, Varisco M, Rajacic Z, Vosbeck J, et al. Preventing implant-associated infections by silver coating. *Antimicrob Agents Chemother*. 2016;**60**(4):2467–75. doi: [10.1128/AAC.02934-15](https://doi.org/10.1128/AAC.02934-15). [PubMed: [26883700](https://pubmed.ncbi.nlm.nih.gov/26883700/)]. [PubMed Central: [PMC4808148](https://pubmed.ncbi.nlm.nih.gov/PMC4808148/)].
- Obeng-Nkrumah N, Labi AK, Acquah ME, Donkor ES. Bloodstream infections in patients with malignancies: Implications for antibiotic treatment in a Ghanaian tertiary setting. *BMC Res Notes*. 2015;**8**:742. doi: [10.1186/s13104-015-1701-z](https://doi.org/10.1186/s13104-015-1701-z). [PubMed: [26628056](https://pubmed.ncbi.nlm.nih.gov/26628056/)]. [PubMed Central: [PMC4667459](https://pubmed.ncbi.nlm.nih.gov/PMC4667459/)].
- Tao F, Jiang R, Chen Y, Chen R. Risk factors for early onset of catheter-related bloodstream infection in an intensive care unit in China: A retrospective study. *Med Sci Monit*. 2015;**21**:550–6. doi: [10.12659/MSM.892121](https://doi.org/10.12659/MSM.892121). [PubMed: [25695128](https://pubmed.ncbi.nlm.nih.gov/25695128/)]. [PubMed Central: [PMC4343039](https://pubmed.ncbi.nlm.nih.gov/PMC4343039/)].
- Oliveira WF, Silva PMS, Silva RCS, Silva GMM, Machado G, Coelho L, et al. Staphylococcus aureus and Staphylococcus epidermidis infections on implants. *J Hosp Infect*. 2018;**98**(2):111–7. doi: [10.1016/j.jhin.2017.11.008](https://doi.org/10.1016/j.jhin.2017.11.008). [PubMed: [29175074](https://pubmed.ncbi.nlm.nih.gov/29175074/)].
- Mekni MA, Bouchami O, Achour W, Ben Hassen A. Strong biofilm production but not adhesion virulence factors can discriminate between invasive and commensal Staphylococcus epidermidis strains. *APMIS*. 2012;**120**(8):605–11. doi: [10.1111/j.1600-0463.2012.02877.x](https://doi.org/10.1111/j.1600-0463.2012.02877.x). [PubMed: [22779682](https://pubmed.ncbi.nlm.nih.gov/22779682/)].
- Cerca N, Jefferson KK, Oliveira R, Pier GB, Azeredo J. Comparative antibody-mediated phagocytosis of Staphylococcus epidermidis cells grown in a biofilm or in the planktonic state. *Infect Immun*. 2006;**74**(8):4849–55. doi: [10.1128/IAI.00230-06](https://doi.org/10.1128/IAI.00230-06). [PubMed: [16861673](https://pubmed.ncbi.nlm.nih.gov/16861673/)]. [PubMed Central: [PMC1539625](https://pubmed.ncbi.nlm.nih.gov/PMC1539625/)].
- Cerca N, Jefferson KK, Maira-Litran T, Pier DB, Kelly-Quintos C, Goldmann DA, et al. Molecular basis for preferential protective efficacy of antibodies directed to the poorly acetylated form of staphylococcal poly-N-acetyl-beta-(1-6)-glucosamine. *Infect Immun*. 2007;**75**(7):3406–13. doi: [10.1128/IAI.00078-07](https://doi.org/10.1128/IAI.00078-07). [PubMed: [17470540](https://pubmed.ncbi.nlm.nih.gov/17470540/)]. [PubMed Central: [PMC1932961](https://pubmed.ncbi.nlm.nih.gov/PMC1932961/)].
- Kristian SA, Birkenstock TA, Sauder U, Mack D, Gotz F, Landmann R. Biofilm formation induces C3a release and protects Staphylococcus epidermidis from IgG and complement deposition and from neutrophil-dependent killing. *J Infect Dis*. 2008;**197**(7):1028–35. doi: [10.1086/528992](https://doi.org/10.1086/528992). [PubMed: [18419540](https://pubmed.ncbi.nlm.nih.gov/18419540/)].
- Harris LG, Murray S, Pascoe B, Bray J, Meric G, Mageiros L, et al. Biofilm morphotypes and population structure among Staphylococcus epidermidis from commensal and clinical samples. *PLoS One*. 2016;**11**(3):e0151240. doi: [10.1371/journal.pone.0151240](https://doi.org/10.1371/journal.pone.0151240). [PubMed: [26978068](https://pubmed.ncbi.nlm.nih.gov/26978068/)]. [PubMed Central: [PMC4792440](https://pubmed.ncbi.nlm.nih.gov/PMC4792440/)].
- Su CY, Ming QL, Rahman K, Han T, Qin LP. Salvia miltiorrhiza: Traditional medicinal uses, chemistry, and pharmacology. *Chin J Nat Med*. 2015;**13**(3):163–82. doi: [10.1016/S1875-5364\(15\)30002-9](https://doi.org/10.1016/S1875-5364(15)30002-9). [PubMed: [25835361](https://pubmed.ncbi.nlm.nih.gov/25835361/)].
- Xu J, Wei K, Zhang G, Lei L, Yang D, Wang W, et al. Ethnopharmacology, phytochemistry, and pharmacology of Chinese Salvia species: A review. *J Ethnopharmacol*. 2018;**225**:18–30. doi: [10.1016/j.jep.2018.06.029](https://doi.org/10.1016/j.jep.2018.06.029). [PubMed: [29935346](https://pubmed.ncbi.nlm.nih.gov/29935346/)].
- Takahashi K, Ouyang X, Komatsu K, Nakamura N, Hattori M, Baba A, et al. Sodium tanshinone IIA sulfonate derived from Danshen (*Salvia miltiorrhiza*) attenuates hypertrophy induced by angiotensin II in cultured neonatal rat cardiac cells. *Biochem Pharmacol*. 2002;**64**(4):745–9. doi: [10.1016/S0006-2952\(02\)01250-9](https://doi.org/10.1016/S0006-2952(02)01250-9). [PubMed: [12167494](https://pubmed.ncbi.nlm.nih.gov/12167494/)].
- Maione F, Cantone V, Chini MG, De Feo V, Mascolo N, Bifulco G. Molecular mechanism of tanshinone IIA and cryptotanshinone in platelet anti-aggregating effects: An integrated study of pharmacology and computational analysis. *Fitoterapia*. 2015;**100**:174–8. doi: [10.1016/j.fitote.2014.11.024](https://doi.org/10.1016/j.fitote.2014.11.024). [PubMed: [25497578](https://pubmed.ncbi.nlm.nih.gov/25497578/)].
- Bissinger R, Lupescu A, Zelenak C, Jilani K, Lang F. Stimulation of eryptosis by cryptotanshinone. *Cell Physiol Biochem*. 2014;**34**(2):432–42. doi: [10.1159/000363012](https://doi.org/10.1159/000363012). [PubMed: [25095724](https://pubmed.ncbi.nlm.nih.gov/25095724/)].
- Dominguez More GP, Cardenas PA, Costa GM, Simoes CMO, Aragon DM. Pharmacokinetics of botanical drugs and plant extracts. *Mini Rev Med Chem*. 2017;**17**(17):1646–64. doi: [10.2174/1389557517666170510112508](https://doi.org/10.2174/1389557517666170510112508). [PubMed: [28494732](https://pubmed.ncbi.nlm.nih.gov/28494732/)].
- Jamshidi-Aidji M, Morlock GE. From bioprofiling and characterization to bioquantification of natural antibiotics by direct bioautography linked to high-resolution mass spectrometry: Exemplarily shown for salvia miltiorrhiza root. *Anal Chem*. 2016;**88**(22):10979–86. doi: [10.1021/acs.analchem.6b02648](https://doi.org/10.1021/acs.analchem.6b02648). [PubMed: [27766834](https://pubmed.ncbi.nlm.nih.gov/27766834/)].
- Cha JD, Lee JH, Choi KM, Choi SM, Park JH. Synergistic effect between cryptotanshinone and antibiotics against clinic methicillin and vancomycin-resistant Staphylococcus aureus. *Evid Based Complement Alternat Med*. 2014;**2014**:450572. doi: [10.1155/2014/450572](https://doi.org/10.1155/2014/450572). [PubMed: [24782909](https://pubmed.ncbi.nlm.nih.gov/24782909/)]. [PubMed Central: [PMC3982256](https://pubmed.ncbi.nlm.nih.gov/PMC3982256/)].
- Lee DS, Lee SH, Noh JG, Hong SD. Antibacterial activities of cryptotanshinone and dihydrotanshinone I from a medicinal herb, Salvia miltiorrhiza Bunge. *Biosci Biotechnol Biochem*. 1999;**63**(12):2236–9. doi: [10.1271/bbb.63.2236](https://doi.org/10.1271/bbb.63.2236). [PubMed: [10664860](https://pubmed.ncbi.nlm.nih.gov/10664860/)].
- Feng H, Xiang H, Zhang J, Liu G, Guo N, Wang X, et al. Genome-wide transcriptional profiling of the response of Staphylococcus aureus to cryptotanshinone. *J Biomed Biotechnol*. 2009;**2009**:617509. doi: [10.1155/2009/617509](https://doi.org/10.1155/2009/617509). [PubMed: [19707532](https://pubmed.ncbi.nlm.nih.gov/19707532/)]. [PubMed Central: [PMC2730559](https://pubmed.ncbi.nlm.nih.gov/PMC2730559/)].
- Hui YI, Ruiling ZU, Yuling YI, Yan LI. [Inhibitory effect of cryptotanshinone on biofilm of Staphylococcus epidermidis]. *Chin J infect Control*. 2017;**16**(9):798–803. Chinese.
- Wu Y, Wu Y, Zhu T, Han H, Liu H, Xu T, et al. Staphylococcus epidermidis SrrAB regulates bacterial growth and biofilm formation differently under oxic and microaerobic conditions. *J Bacteriol*. 2015;**197**(3):459–76. doi: [10.1128/JB.02231-14](https://doi.org/10.1128/JB.02231-14). [PubMed: [25404696](https://pubmed.ncbi.nlm.nih.gov/25404696/)]. [PubMed Central: [PMC4285975](https://pubmed.ncbi.nlm.nih.gov/PMC4285975/)].
- Govantes F. Serial dilution-based growth curves and growth curve synchronization for high-resolution time series of bacterial biofilm growth. *Methods Mol Biol*. 2018;**1734**:159–69. doi: [10.1007/978-1-4939-7604-1\\_13](https://doi.org/10.1007/978-1-4939-7604-1_13). [PubMed: [29288453](https://pubmed.ncbi.nlm.nih.gov/29288453/)].
- Shi C, Li M, Muhammad I, Ma X, Chang Y, Li R, et al. Combination of berberine and ciprofloxacin reduces multi-resistant Salmonella strain biofilm formation by depressing mRNA expressions of luxS, rpoE, and ompR. *J Vet Sci*. 2018;**19**(6):808–16. doi: [10.4142/jvs.2018.19.6.808](https://doi.org/10.4142/jvs.2018.19.6.808). [PubMed: [30304890](https://pubmed.ncbi.nlm.nih.gov/30304890/)]. [PubMed Central: [PMC6265579](https://pubmed.ncbi.nlm.nih.gov/PMC6265579/)].
- Field D, Gaudin N, Lyons F, O'Connor PM, Cotter PD, Hill C, et al. A bioengineered nisin derivative to control biofilms of Staphylococcus pseudintermedius. *PLoS One*. 2015;**10**(3):e0119684. doi: [10.1371/journal.pone.0119684](https://doi.org/10.1371/journal.pone.0119684). [PubMed: [25789988](https://pubmed.ncbi.nlm.nih.gov/25789988/)]. [PubMed Central: [PMC4366236](https://pubmed.ncbi.nlm.nih.gov/PMC4366236/)].
- Silva S, Henriques M, Martins A, Oliveira R, Williams D, Azeredo J. Biofilms of non-Candida albicans Candida species: Quantification, structure and matrix composition. *Med Mycol*. 2009;**47**(7):681–9. doi: [10.3109/13693780802549594](https://doi.org/10.3109/13693780802549594). [PubMed: [19888800](https://pubmed.ncbi.nlm.nih.gov/19888800/)].

26. Clinical and Laboratory Standards Institute. *Methods for dilution antimicrobial susceptibility tests for bacteria that grow aerobically: Approved standard. M100*. Clinical and Laboratory Standards Institute; 2017.
27. Labthavikul P, Petersen PJ, Bradford PA. In vitro activity of tigecycline against *Staphylococcus epidermidis* growing in an adherent-cell biofilm model. *Antimicrob Agents Chemother*. 2003;**47**(12):3967–9. doi: [10.1128/AAC.47.12.3967-3969.2003](https://doi.org/10.1128/AAC.47.12.3967-3969.2003). [PubMed: [14638511](https://pubmed.ncbi.nlm.nih.gov/14638511/)]. [PubMed Central: [PMC296180](https://pubmed.ncbi.nlm.nih.gov/PMC296180/)].
28. Macia MD, Rojo-Molinero E, Oliver A. Antimicrobial susceptibility testing in biofilm-growing bacteria. *Clin Microbiol Infect*. 2014;**20**(10):981–90. doi: [10.1111/1469-0691.12651](https://doi.org/10.1111/1469-0691.12651). [PubMed: [24766583](https://pubmed.ncbi.nlm.nih.gov/24766583/)].
29. Dong Y, Chen S, Wang Z, Peng N, Yu J. Synergy of ultrasound microbubbles and vancomycin against *Staphylococcus epidermidis* biofilm. *J Antimicrob Chemother*. 2013;**68**(4):816–26. doi: [10.1093/jac/dks490](https://doi.org/10.1093/jac/dks490). [PubMed: [23248238](https://pubmed.ncbi.nlm.nih.gov/23248238/)].
30. Gonzalez-Ramirez AI, Ramirez-Granillo A, Medina-Canales MG, Rodriguez-Tovar AV, Martinez-Rivera MA. Analysis and description of the stages of *Aspergillus fumigatus* biofilm formation using scanning electron microscopy. *BMC Microbiol*. 2016;**16**(1):243. doi: [10.1186/s12866-016-0859-4](https://doi.org/10.1186/s12866-016-0859-4). [PubMed: [27756222](https://pubmed.ncbi.nlm.nih.gov/27756222/)]. [PubMed Central: [PMC5069814](https://pubmed.ncbi.nlm.nih.gov/PMC5069814/)].
31. Otto M. Molecular basis of *Staphylococcus epidermidis* infections. *Semin Immunopathol*. 2012;**34**(2):201–14. doi: [10.1007/s00281-011-0296-2](https://doi.org/10.1007/s00281-011-0296-2). [PubMed: [22095240](https://pubmed.ncbi.nlm.nih.gov/22095240/)]. [PubMed Central: [PMC3272124](https://pubmed.ncbi.nlm.nih.gov/PMC3272124/)].
32. Yue J, Yang H, Liu S, Song F, Guo J, Huang C. Influence of naringenin on the biofilm formation of *Streptococcus mutans*. *J Dent*. 2018;**76**:24–31. doi: [10.1016/j.jdent.2018.04.013](https://doi.org/10.1016/j.jdent.2018.04.013). [PubMed: [29679633](https://pubmed.ncbi.nlm.nih.gov/29679633/)].
33. El-Gharbaoui A, Benitez G, Gonzalez-Tejero MR, Molero-Mesa J, Merzouki A. Comparison of Lamiaceae medicinal uses in eastern Morocco and eastern Andalusia and in Ibn al-Baytar's compendium of simple medicaments (13th century CE). *J Ethnopharmacol*. 2017;**202**:208–24. doi: [10.1016/j.jep.2017.03.014](https://doi.org/10.1016/j.jep.2017.03.014). [PubMed: [28323048](https://pubmed.ncbi.nlm.nih.gov/28323048/)].
34. Rohde H, Frankenberger S, Zahringer U, Mack D. Structure, function and contribution of polysaccharide intercellular adhesin (PIA) to *Staphylococcus epidermidis* biofilm formation and pathogenesis of biomaterial-associated infections. *Eur J Cell Biol*. 2010;**89**(1):103–11. doi: [10.1016/j.ejcb.2009.10.005](https://doi.org/10.1016/j.ejcb.2009.10.005). [PubMed: [19913940](https://pubmed.ncbi.nlm.nih.gov/19913940/)].
35. Singh VK. High level expression and purification of atl, the major autolytic protein of *Staphylococcus aureus*. *Int J Microbiol*. 2014;**2014**:615965. doi: [10.1155/2014/615965](https://doi.org/10.1155/2014/615965). [PubMed: [24669224](https://pubmed.ncbi.nlm.nih.gov/24669224/)]. [PubMed Central: [PMC3941666](https://pubmed.ncbi.nlm.nih.gov/PMC3941666/)].
36. Yu D, Zhao L, Xue T, Sun B. *Staphylococcus aureus* autoinducer-2 quorum sensing decreases biofilm formation in an icaR-dependent manner. *BMC Microbiol*. 2012;**12**:288. doi: [10.1186/1471-2180-12-288](https://doi.org/10.1186/1471-2180-12-288). [PubMed: [23216979](https://pubmed.ncbi.nlm.nih.gov/23216979/)]. [PubMed Central: [PMC3539994](https://pubmed.ncbi.nlm.nih.gov/PMC3539994/)].
37. Niu C, Robbins CM, Pittman KJ, Osborn J L, Stubblefield BA, Simmons RB, et al. LuxS influences *Escherichia coli* biofilm formation through autoinducer-2-dependent and autoinducer-2-independent modalities. *FEMS Microbiol Ecol*. 2013;**83**(3):778–91. doi: [10.1111/1574-6941.12034](https://doi.org/10.1111/1574-6941.12034). [PubMed: [23078586](https://pubmed.ncbi.nlm.nih.gov/23078586/)].
38. Singh R, Ray P. Quorum sensing-mediated regulation of staphylococcal virulence and antibiotic resistance. *Future Microbiol*. 2014;**9**(5):669–81. doi: [10.2217/fmb.14.31](https://doi.org/10.2217/fmb.14.31). [PubMed: [24957093](https://pubmed.ncbi.nlm.nih.gov/24957093/)].